IEEE Access
Multidisciplinary | Rapid Review | Open Access Journal

Received March 12, 2020, accepted April 3, 2020, date of publication April 27, 2020, date of current version May 12, 2020.

Digital Object Identifier 10.1109/ACCESS.2020.2990581

Research on Modeling and the Operation Strategy of a Hydrogen-Battery Hybrid Energy Storage System for Flexible Wind Farm Grid-Connection

TING WEN[1], ZHEYUAN ZHANG[2], XIANGNING LIN[1], (Senior Member, IEEE), ZHENGTIAN LI[1], CHONG CHEN[3], AND ZHIXUN WANG[1]

[1]State Key Laboratory of Advanced Electromagnetic Engineering and Technology, Huazhong University of Science and Technology, Wuhan 430074, China
[2]Powerchina Hubei Electric Engineering Corporation Limited, Wuhan 430040, China
[3]Changjiang Institute of Survey, Planning, Design, and Research, Wuhan 430010, China

Corresponding author: Zhengtian Li (lizhengtian@hust.edu.cn)

This work was supported in part by the National Natural Science Foundation of China under Grant 51537003, and in part by the Science and Technology Project of State Grid Corporation of China under Grant 5700-20199495A-0-0-00.

ABSTRACT Energy storage systems used for the flexible grid connection of wind farms in terms of minute time-scale usually consist of batteries. Due to the capacity constraints of batteries, when wind energy fluctuations exceed limits continuously, this type of energy storage system topology cannot present good performance. To solve this problem, this paper introduces a hybrid energy storage system (HESS) topology consisting of batteries and a hydrogen conversion system (HCS). To achieve a flexible wind farm grid connection with a minimum energy loss, a HESS control strategy is proposed to make full use of the advantages of the HCS capacity and battery energy conversion efficiency. The optimization goal is to minimize power fluctuations, battery life consumption, and energy loss. The energy conversion characteristics of the flexible wind farm grid-connection system are also analyzed. The simulation results show that compared with other strategies using only batteries, the operating strategy using the HESS with the same cost can combine the advantages of the battery efficiency and HCS power continuity to achieve a balance between the controlling energy loss and smoothing power fluctuations.

INDEX TERMS Hydrogen conversion system, smoothing power fluctuations, hybrid energy storage system, flexible wind farm grid-connection.

I. INTRODUCTION

Wind power has been widely used due to its clean and environmentally friendly characteristics. However, the stochastic volatility characteristics of wind power lead the power fluctuations of wind power to exceed the grid-connection regulations. If the wind power is not flexibly connected to the grid, the power system dispatching and safe operation will be threatened [1], [2]. Regulations of power connected to the power grid are published in many countries. The Irish ESB company [3] advises that the active power output change limit is 5% of the installed capacity within arbitrary 15 minutes when the installed capacity is less than 100 MW, 4% when the installed capacity is less than 200 MW, and 2% when the installed capacity is greater than 200 MW.

The associate editor coordinating the review of this manuscript and approving it for publication was Giambattista Gruosso.

With the continuous development of energy storage technology, research on the use of energy storage systems in conjunction with flexible grid-connected control schemes has yielded many fruitful early results. As shown in [4] and [5], a hybrid energy storage system is proposed, consisting of a super capacitor and a hydrogen storage device, which are used to stabilize the grid-connected power of wind power and DC bus voltage fluctuations on the second-level timescale. Reference [6]–[8] has proposed to decompose wind power fluctuations on two different timescales: second-level and minute-level. Then, a hybrid energy storage system consisting of super capacitors and batteries is used to stabilize power fluctuations on two timescales. In addition, some literature focus on grid-connected fluctuation power on the minute-level timescale, and battery life is also considered. As shown in [9], the model predictive control idea is used to control the battery to participate in the flexible grid-connection on the

This work is licensed under a Creative Commons Attribution 4.0 License. For more information, see https://creativecommons.org/licenses/by/4.0/

minute timescale. As shown in [10], to prevent the battery from over charging and discharging, the state of charge (SOC) feedback regulates the charging filtering parameters of the battery. The battery output is reduced to prevent overcharging when the SOC is too high. The reference [11] expounds the concept and structure of wind-hydrogen coupled power generation and demonstrates the feasibility of a hydrogen storage system participating in the flexible wind farm grid-connection at the minute timescale.

The above-mentioned research lays a solid foundation for wind farm power fluctuation suppression and energy storage system control strategies. However, the above-mentioned research has not considered the following two aspects: first, in terms of the energy storage structure, the above-mentioned research mainly uses a single battery or hydrogen energy storage device to suppress the power fluctuation in a minute timescale. However, the control ability of the battery for flexible wind farm grid-connections is limited by the SOC when the budget is limited, so it is difficult to meet the needs of continuously increasing or decreasing wind power. When the cost of the hydrogen storage system is fixed, the capacity of the hydrogen storage unit can be allocated reasonably. Then, the hydrogen storage capacity can be considered to be enough to meet the dispatching requirements within 24 hours of the intraday dispatching period, and the flexible grid-connection problem caused by the capacity limits can be well solved. However, compared with batteries, the energy conversion efficiency of hydrogen storage devices is relatively low, and the cost is relatively high [11], [12]. To solve the above-mentioned problems and by considering the energy storage system structure commonly used in wind farms, the hybrid energy storage system is composed of a hydrogen storage unit and batteries. The former can be considered to have an unlimited capacity in the intraday dispatching timescale, and the latter has a low energy conversion loss. In this way, the round-the-clock and highly efficient flexible grid connection of wind power is achieved. Second, in terms of the operational control objective, the above-mentioned studies mainly focus on how to maximize the smooth grid-connected power of wind power without optimizing the energy loss generated by the energy storage system in the process of energy conversion. This loss is only considered in modeling the energy storage system. In this way, it is difficult to globally optimize the output smoothing index and the operating cost of the energy storage system. Therefore, the ideal effect of balancing the output fluctuation control effect and the cost of energy conversion are hard to achieve.

Therefore, this paper studies the topology of a battery-hydrogen hybrid energy storage system. By constructing a comprehensive objective function that considers the fluctuation of grid-connected power, the smoothness of the energy storage output and energy loss, a flexible grid-connected control strategy of wind power is proposed. This strategy effectively improves the continuity of the power supply by using a hydrogen energy storage system in the timescale of intraday dispatching, and a model for evaluating the energy conversion characteristics of energy storage is established. Then, this paper quantitatively evaluated the overall energy conversion characteristics of the hybrid energy storage system after the implementation of the control strategy. The effects of the energy storage system ratio and the penalty factor on the control results are studied. Both the theoretical analysis and case study prove the effectiveness and superiority of the proposed system scheme, optimization model and energy consumption evaluation model.

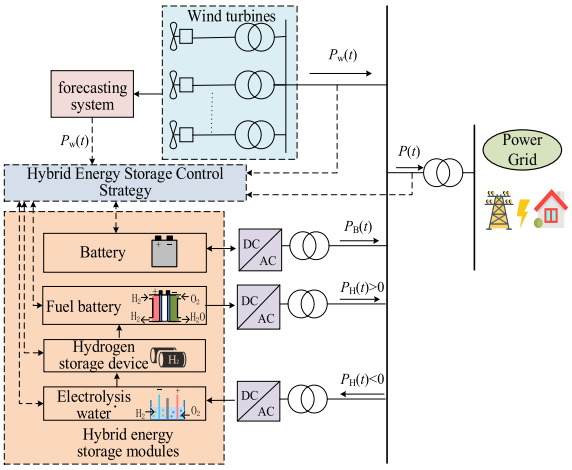

FIGURE 1. Wind-battery-hydrogen system control block.

II. SYSTEM MODELING

Fig. 1 shows the topological structure of the wind-storage-hydrogen co-generation system. Let t be any time in the operation cycle. $P_W(t)$ is the original active power output by wind turbines. $P(t)$ is the grid-connected power of the combined system. $P_B(t)$ represents the charging and discharging power of the battery, and it is recorded as $P_B(t) < 0$ when charging and $P_B(t) > 0$ when discharging. $P_H(t)$ represents the charging and discharging power of the hydrogen energy storage system. $P_H(t) < 0$ represents the electrolytic cells absorbing the active power. $P_H(t) > 0$ represents the fuel cells releasing active power. The real-time balance expression of the active power of a wind farm is shown in (1).

$$P(t) = P_W(t) + P_B(t) + P_H(t) \tag{1}$$

A. HYBRID ENERGY STORAGE MODULES

1) SYSTEM CHARACTERISTICS MODELING

The residual energy $E_B(t)$ of the battery is shown in (2), and the SOC of the battery is shown in (3).

$$E_B(t) = \begin{cases} E_B(t-\Delta t) - P_B(t)\cdot\Delta t\cdot\eta_{Bc}, & P_B(t) < 0 \\ E_B(t-\Delta t) - P_B(t)\cdot\Delta t/\eta_{Bd}, & P_B(t) > 0 \end{cases} \tag{2}$$

$$S_{SOC}(t) = \frac{E_B(t)}{E_{bm}} \times 100\% \tag{3}$$

where Δt is the dispatching period, that is, 15 minutes, η_{Bc} and η_{Bd} represent the charging and discharging efficiencies

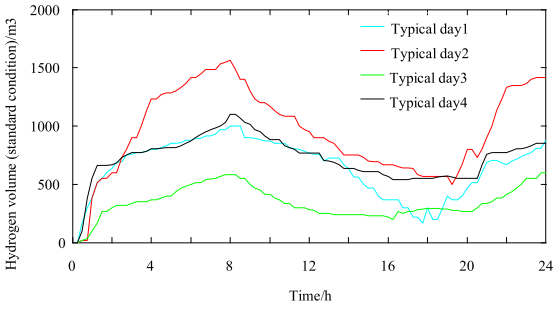

FIGURE 2. The volume of hydrogen on four typical days.

of the batteries, respectively, which are 90%, and E_{bm} is the rated capacity of the batteries.

Hydrogen production ΔW_{H} by a water electrolysis hydrogen plant under standard conditions and the input electric quantity of the water electrolysis device [13] are shown in (4).

$$\Delta W_{\mathrm{H}} = P_{\mathrm{H}}(t) \cdot \Delta t \cdot \eta_{\mathrm{Hc}} \tag{4}$$

$$\eta_{\mathrm{Hc}} = \frac{N_{\mathrm{H_2,out}} \cdot H_{\mathrm{HHV}}}{P_{\mathrm{H}} + Q_{\mathrm{cell}}(1 - T_0/T_{\mathrm{s}}) + Q_{\mathrm{H_2O}}(1 - T_0/T_{\mathrm{s}})} \tag{5}$$

where η_{Hc} represents the electro-hydrogen conversion ratio of the electrolytic device, P_{H} represents the operating power, and H_{HHV} represents the calorific value of hydrogen, which is 284.7 kJ/mol. $N_{\mathrm{H2,out}}$ represents the rate of hydrogen production, that is, 0.05 mol/s, η_{total} represents the heat energy provided by the external heat source, that is, 0.23 kJ/s, and $Q_{\mathrm{H_2O}}$ represents the energy required to heat water, that is, 0.47 kJ/s. T_0 and T_{s} represent the ambient temperature and the temperature of the heating source, respectively, that is, 298.15 K and 873.15 K, respectively.

When the mass of hydrogen ΔW_{H} is known, the total energy released by the hydrogen fuel cell G3000 [14] can be calculated by (6):

$$P_{\mathrm{H}}(t) \cdot \Delta t = \eta_{\mathrm{Hd}} \cdot \Delta W_{\mathrm{H}}, \quad \eta_{\mathrm{Hd}} = \frac{\rho_0 U_{\mathrm{H}}}{\rho p_{\mathrm{cs}} A} \Delta W_{\mathrm{H}} \tag{6}$$

where η_{Hd} represents the hydrogen-to-electricity conversion ratio of the fuel cell, and U_{H} represents the output voltage of the fuel cell, that is, 500 V. ρ and ρ_0 represent the hydrogen gas density at 273 K/81.04 MPa and standard conditions, respectively, which are 38 g/L and 0.0899 g/L. p_{cs} represents the number of single cells in the stack cells, that is, 640. The coefficient A is 0.42.

By using the measured data of a 100 MW wind farm (with 10 MW batteries) in China, replacing its batteries with a hydrogen energy storage system of the same rated power [8], together with the current control strategy for smoothing fluctuations, the curves of the hydrogen volume under standard conditions on 4 typical days of 4 different seasons are shown in Fig. 2.

As shown in Fig. 2, the maximum possible value of hydrogen produced in one day is less than 1600 m^3 for the wind farm mentioned above. Meanwhile, a unit volume (1 m^3) of a hydrogen storage tank under an 81.04 MPa pressure can accommodate 400 m^3 hydrogen under standard conditions. To draw a conclusion from Fig. 2, a hydrogen storage tank of 4 m^3 capacity is able to meet the hydrogen storage demand of intraday dispatching for a wind farm of installed capacity no more than 100MW. As for the case study in Section IV, the capacity of the wind farm exactly matches the above example wind farm. Therefore, the hydrogen tank of 4 m^3 is sufficient enough to satisfy the adjusting requirement. Thus, in the following, a hydrogen storage tank of a 4 m^3 capacity is adopted. By this arrangement, the upper limit of the hydrogen reserve tank does not need to be considered specifically because the installed capacity of the investigated wind farm in the section of the case study is no more than 100MW (exactly equal to 100 MW).

2) ECONOMIC ANALYSIS OF THE HYBRID ENERGY STORAGE SYSTEM

At present, the control strategy used to suppress wind power fluctuations mainly acts on the battery. Whereas, the control strategy proposed in this paper acts on the hybrid energy storage system, including the battery and hydrogen energy storage device. To make the control effect more convincing, the two kinds of energy storage systems should have the same allocation cost. Ref. [15] points out that for 100 MW wind farms, it is recommended to use batteries with a rated power of 10 MW and a rated capacity of 10 MWh. The cost of this recommended system is approximately 26 million yuan. Ref. [16] points out that the cost per unit power of the hydrogen storage system is approximately twice that of the battery. The cost of a hybrid energy storage system consisting of a 6 MW battery and 2 MW hydrogen storage equipment is the same as that of the above-mentioned pure battery energy storage system. In addition, after inquiry, the cost of a 4 m^3 hydrogen storage tank is approximately 160,000 yuan. Therefore, the cost of the energy storage system consisting of 6 MW batteries and 2 MW hydrogen storage equipment is the same as that of 10 MW batteries. The following discussion is based on the above-mentioned allocation.

B. HYBRID ENERGY STORAGE CONTROL MODULE

By using the rolling optimization idea of the predictive control model, the latest ultra-short-term wind power forecasting data, the grid-connected power of a wind farm and the energy state of the hybrid energy storage system acquired in real-time are input into the hybrid energy storage control module. The finite time-domain optimization problem defined in Section III is solved online to obtain the charging and discharging power of the hybrid energy storage system in this dispatching period, and only the results of the first step are output. Then, the whole system loops again.

C. WIND POWER FORECASTING MODULE

The data of the wind farms described in Section A are obtained. The wind power forecasting algorithm described in reference [17]–[20] is used to forecast wind power with

timescales of 15 minutes and 3 hours. The forecasting results are normalized and evaluated. The extreme learning machine (ELM) algorithm with slightly better evaluation results is selected, and the forecast period is 3 hours and updated with time. The sampling timescale and scheduling timescale of hybrid energy storage are set to 15 minutes.

III. POWER FLUCTUATION SUPPRESSION STRATEGY OF HYBRID ENERGY STORAGE

A. DEFINITION OF THE EVALUATION INDEX

1) OVER-LIMIT INDEX OF THE POWER FLUCTUATION IN THE GRID-CONNECTION

The over-limit amplitude ΔP_s of the active power fluctuation in the wind farm grid-connection is shown in (7)

$$\Delta P_S = [\sum_{k=1}^{T/\Delta t-1} (\max\{\Delta P(t+k\Delta t) - D_{et}, 0\})^2 + (\min\{\Delta P(t+k\Delta t) + D_{et}, 0\})^2]^{1/2} \quad (7)$$

$$\Delta P(t) = P(t) - P(t-\Delta t) \quad (8)$$

where T is the operation period, set as 3 hours, and D_{et} is the allowable value of the fluctuating power for the grid-connection, set as 2 MW.

2) TOTAL CHARGE AND DISCHARGE INDEX OF BATTERIES

The aging condition of a battery [21] when it irregularly fluctuates with the wind farm grid-connected power can be expressed as

$$\delta = \sum_{i=1}^{3} \varepsilon_i \left(\sum_{k=1}^{T_c} \frac{|P_B(t+k\Delta t)| \cdot \Delta t}{U_B(t+k\Delta t)} \right)^z \quad (9)$$

where ε_i is a constant representing the characteristics of the batteries, T_c is the total time of charging and discharging the batteries, and U_B is the working voltage of the batteries. It can be seen that the smaller the total charge and discharge power in the whole life cycle, the lighter the life aging status of the batteries. To reduce the life cycle loss, the total charge and discharge index of the battery is set up as shown in (10):

$$\delta_{P_B} = \sqrt{\sum_{k=1}^{T/\Delta t-1} (\Delta t \cdot P_B(t+k\Delta t))^2} \quad (10)$$

The maximum discharge depth also affects the life of the battery. Therefore, the maximum discharge depth is set as a constraint in this paper, which can be seen in Part B.

3) ENERGY LOSS INDEX

When the wind power is sharply increasing, the wind energy curtailment $\Delta E_{dis}(t)$ is obtained by integrating the wind power curtailment with time, as shown in (11).

$$\Delta E_{dis}(t) = \Delta t \cdot \max\{\Delta P(t) - D_{et}, 0\} \quad (11)$$

There is an energy conversion loss in the charge-discharge process of hybrid energy storage systems. The energy conversion losses of batteries $\Delta E_B(t)$ and hydrogen storage systems $\Delta E_H(t)$ are shown in (12) and (13).

$$\Delta E_B(t) = \begin{cases} -P_B(t) \cdot \Delta t \cdot (1-\eta_{Bc}), & P_B(t) < 0 \\ P_B(t) \cdot \Delta t \cdot (1/\eta_{Bd} - 1), & P_B(t) > 0 \end{cases} \quad (12)$$

$$\Delta E_H(t) = \begin{cases} -P_H(t) \cdot \Delta t \cdot (1-\eta_{Hc}), & P_H(t) < 0 \\ P_H(t) \cdot \Delta t \cdot (1/\eta_{Hd} - 1), & P_H(t) > 0 \end{cases} \quad (13)$$

The energy loss index $\Delta E(t)$ is shown in (14).

$$\Delta E(t) = [\sum_{k=1}^{T/\Delta t-1} (\Delta E_{dis}(t+k\Delta t) + \Delta E_B(t+k\Delta t) + \Delta E_H(t+k\Delta t))^2]^{1/2} \quad (14)$$

B. MODELING THE HYBRID ENERGY STORAGE CONTROL SYSTEM

1) OBJECTIVE FUNCTION

The penalty coefficients α and β are used to convert the three optimization objective functions shown in (7), (10) and (14) into a single objective optimization problem. The objective functions are listed as follows:

$$\min J = \Delta P_s + \alpha \delta_{P_B} + \beta \Delta E \quad (15)$$

2) CONSTRAINTS

The charging-discharging power and residual energy of batteries satisfies the constraints (16) and (17).

$$P_{Bcm} \le P_B(t) \le P_{Bdm} \quad (16)$$

$$E_{b\,min} \le E_B(t) \le E_{b\,max} \quad (17)$$

where P_{Bcm} and P_{Bdm} are the maximal charging and discharging power of the battery. $E_{b\,min}$ and $E_{b\,max}$ are the SOC limit of the battery, which represent the limit of the charge/discharge depth of the battery.

The charging/discharging power of the hydrogen storage system and capacity of the hydrogen tank satisfy the constraints (18) and (19), respectively.

$$P_{Hcm} \le P_H(t) \le P_{Hdm} \quad (18)$$

$$W_H(t) \ge 0 \quad (19)$$

where P_{Hcm} and P_{Hdm} are the rated charging and discharging power of the hydrogen storage system, that is, 2 MW.

3) SOLUTION

The optimization problem is a nonlinear quadratic programming problem, which can be solved by the YALMIP toolbox in MATLAB and the CPLEX solver [22]. The flow chart of the processing is shown in Fig. 3.

C. ENERGY LOSS EVALUATION MODEL OF HYBRID ENERGY STORAGE

For the energy storage system, a more intuitive evaluation index of the energy storage system is defined concerning to the energy conversion efficiency. In the execution process of the control strategy, which is carried out in a flexible wind power grid-connection auxiliary system, the sum of the wind

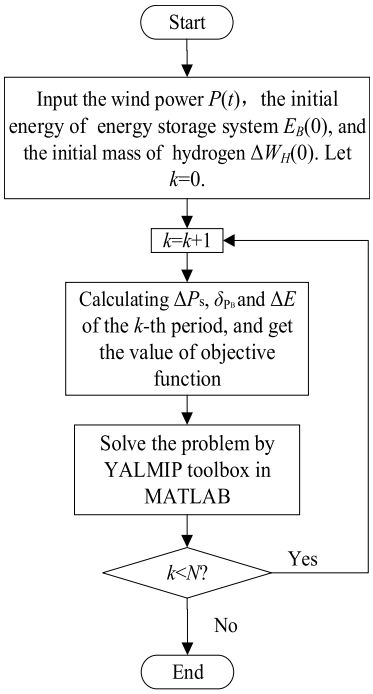

FIGURE 3. The flow chart of the processing.

power fluctuation energy, which exceeds the limit from the initial state, is defined as the cumulative energy $E_{\Delta P}$ of the over-limit power fluctuation, as shown in (20).

$$E_{\Delta P} = \Delta t \sum_{k=1}^{T/\Delta t} \max\{(\Delta P_{\max}(t + k\Delta t) - D_{\text{et}}), 0\} + \min\{\Delta P_{\max}(t + k\Delta t) + D_{\text{et}}, 0\} \quad (20)$$

The energy change of the hybrid energy storage system after charging and discharging from the initial state is defined as $E_{\Delta S}$. The energy storage system has two kinds of energy storage (only the battery and only hydrogen energy storage) to collaborate with three kinds of working modes, as follows. The first mode is when the $E_{\Delta P}$ value is small, in which case the control strategy generally uses only the battery or two kinds of energy storage units together. As the $E_{\Delta P}$ value increases, the control strategy uses only the hydrogen storage energy after the battery is full. The battery works alone and corresponds to the maximum value of the energy change $E_{\Delta S\_h}$. The second mode is when $E_{\Delta P}$ is not higher than the charging energy, corresponding to the rated capacity E_{bm} of the battery, in which $E_{\Delta S\_h}$ is equal to the battery conversion power. When $E_{\Delta P} > E_{\text{bm}}/\eta_{\text{Bc}}$, the battery is full, and the hydrogen storage system starts to work. $E_{\Delta S\_h}$ is equal to the rated capacity of the battery plus some electricity consumed by the hydrogen storage unit, as shown in (21). The third mode is on the contrary: if the mode in which two kinds of energy storage units work at the same time is adopted in the early stage of the fluctuations, the larger the power ratio of the hydrogen storage system, the higher the energy conversion loss. When the hydrogen storage system is charged at the rated power, this situation corresponds to the minimum value $E_{\Delta S\_l}$ of the energy change. When the battery is not full, the two kinds of energy storage units work at the rated power. $E_{\Delta P}$ is allocated according to the power ratio of the two kinds of energy storage units, and $E_{\Delta S\_l}$ is calculated according to the conversion efficiency of the two kinds of energy storage units. When the battery is full, the hydrogen storage unit works alone. $E_{\Delta S\_l}$ is equal to the total converted power of the previous process plus the electricity consumed by storing hydrogen, as shown in (22).

$$E_{\Delta S\_h} = \begin{cases} \eta_{\text{Bc}} \cdot E_{\Delta P}, & E_{\Delta P} \le E_{\text{bm}}/\eta_{\text{Bc}} \\ E_{\text{bm}} + \eta_{\text{Hc}} \cdot (E_{\Delta P} - E_{\text{bm}}/\eta_{\text{Bc}}), & E_{\Delta P} > E_{\text{bm}}/\eta_{\text{Bc}} \end{cases} \quad (21)$$

$$E_{\Delta S\_l} = \begin{cases} \eta_{\text{t}} \cdot E_{\Delta P}, & E_{\Delta P} \le (E_{\text{bm}} + E_{\text{hm}})/\eta_{\text{t}} \\ E_{\text{bm}} + E_{\text{hm}} + \eta_{\text{Hc}} \cdot (E_{\Delta P} - (E_{\text{bm}} + E_{\text{hm}})/\eta_{\text{t}}), & E_{\Delta P} > (E_{\text{bm}} + E_{\text{hm}})/\eta_{\text{t}} \end{cases} \quad (22)$$

The comprehensive energy conversion efficiency η_{total} of the energy storage system is $E_{\Delta S}/E_{\Delta P}$, which indicates the efficiency to consume the total energy when the power fluctuations of the energy storage system exceed the limit.

IV. CASE STUDY

A. STRATEGY COMPARISON AND SIMULATION SCENARIO

To verify the effectiveness of the wind power flexible grid-connected auxiliary system and its optimization model (called Scheme 1), this paper compared it with the control effect of the wind farm grid-connected fluctuation smoothing method [8] (called Scheme 2) by using a battery on a timescale of 15 minutes. The control method of Scheme 2 is as follows: based on the wind power forecasting information, the model prediction method is used to control the power fluctuation of the battery system at the 15 minutes timescale. The objective function includes the optimization of the deviations from ideal SOC values, battery power and grid-connected power fluctuations.

The hybrid energy storage system consists of a 6 MW battery and 2 MW hydrogen storage energy, and the cost is approximately the same as that of Scheme 2 with a 10 MW battery. The total installed capacity of the wind farm is 100 MW. The continuous battery discharge time is 1 h at the rated power, and the initial SOC is set as 30%. Due to the flexible grid connection, reducing fluctuations is the optimization focus of this paper. The penalty coefficient is temporarily set as 0.5 [8]. In practice, it is changed according to the different operational requirements and the tendency of the different indexes.

B. EXECUTION RESULTS OF THE OPTIMIZATION MODEL AND DISCUSSION

1) ANALYSIS OF THE POWER FLUCTUATION SMOOTHING EFFECT

To describe the fluctuation smoothing effect more comprehensively, the number of times that the wind power

TABLE 1. Effects of the different strategies.

Typical days	Scheme	ΔP_s/MW	N_{over}	p_{out}/%	ΔE/(MW·h)
1	No control	22.32	23	23.96	23.24
	②	8.05	4	4.17	7.71
	①	3.21	2	2.08	7.27
2	No control	36.91	31	32.29	39.32
	②	9.75	5	5.21	7.83
	①	2.15	3	3.13	7.18
3	No control	27.98	29	30.21	28.48
	②	8.02	5	5.21	3.82
	①	2.7	1	1.04	3.39
4	No control	37.12	33	34.38	36.86
	②	17.23	9	9.38	15.62
	①	11.29	6	6.25	15.06

fluctuation exceeds the limit N_{over} and the time ratio p_{out} of the over-limit time are set as two indexes, as shown in (23) and (24).

$$N_{over} = \sum_{k=1}^{T/\Delta t-1} S(\max\{\Delta P(t+k\Delta t) - D_{et}, 0\}) + S(\min\{\Delta P(t+k\Delta t) + D_{et}, 0\}) \quad (23)$$

$$p_{out} = \Delta t \cdot N_{over}/T \times 100\% \quad (24)$$

where $S(a) = \begin{cases} 1, & a \neq 0 \\ 0, & a = 0 \end{cases}$

The optimization model of the wind power flexible grid-connection auxiliary system is implemented on 4 typical days of 4 seasons. The amplitude ΔP_s of the over-limit fluctuations, the number of over-limit times N_{over}, the over-limit time ratio p_{out}, and the energy loss index ΔE of the four typical days are listed in Table 1.

It can be seen from Table 1 that the fluctuation smoothing effect of Scheme 1 is much better than that of Scheme 2, and the energy loss of Scheme 1 is smaller too. The average difference between the energy loss indexes of Scheme 2 and Scheme 1 of the four typical days is approximately 0.5 MWh. The wind farm is in the Class II resource area. The current pool purchase price is 0.52 yuan/(kWh). Since 360 days are operationally effective in 1 year, Scheme 1 obtained 93,600 extra yuan of annual grid-connection profit on the energy loss index. The grid-connection power fluctuating curve, the charge/discharge power of the hybrid energy storage system, and the battery SOC curve of typical day 1 are shown in Fig. 4 - Fig. 6, respectively. From these figures, the mechanism of the hybrid energy storage system can be illustrated clearly. For instance, in Fig. 4, it can be observed that the wind power drops down (corresponding to a negative value) sharply at time 20 hour due to an unsatisfactory wind condition. To keep the grid-connection power as stable as possible, the battery immediately releases a large amount of power to compensate the decrease of wind power output, as seen in the Fig. 5(a). Meanwhile, the SOC of the battery decreasing sharply is observed, as seen in Fig. 6.

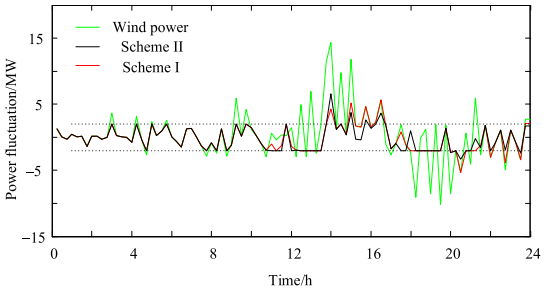

FIGURE 4. The fluctuation of the wind power when connected to the grid.

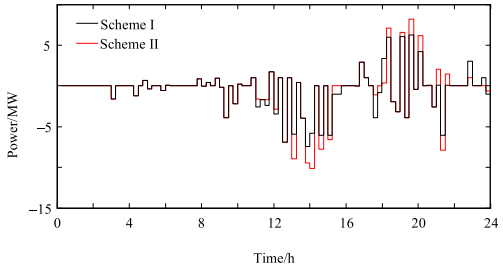

(a) **Battery power**

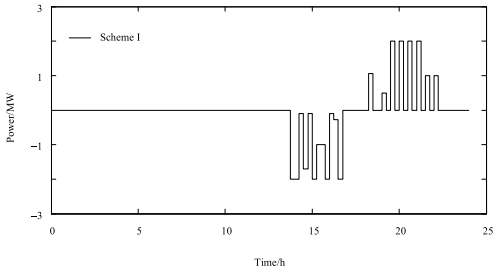

(b) **Power of the hydrogen energy storage device**

FIGURE 5. Power of the hybrid energy storage system.

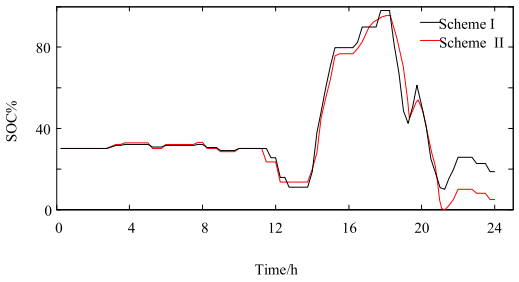

FIGURE 6. SOC curve of the battery.

2) ANALYSIS OF THE EFFECT OF THE GRID-CONNECTION AUXILIARY SYSTEM IN EXTREME CASES

The control effect analysis is carried out by selecting the extreme case where the wind power continuously declined from 80 MW to 20 MW within 2 h. The original power of the wind farm is shown in Fig. 7. The power fluctuation of the grid is shown in Fig. 8. The corresponding over-limit

TABLE 2. Control effect as the wind power sharply declines.

Scheme	ΔP_s/MW	p_{out}/%	ΔE/(MW·h)
Wind power	37.91	49.42	0.84
Scheme ②	16.75	18.98	5.58
Scheme ①	10.15	12.01	7.94

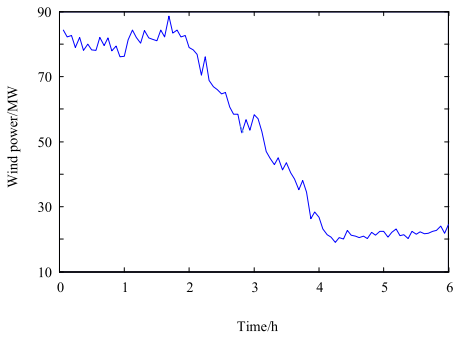

FIGURE 7. Wind power decline.

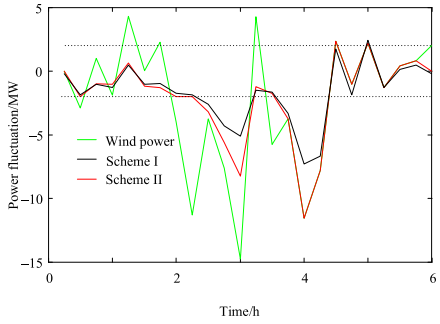

FIGURE 8. Wind power fluctuation.

fluctuation amplitude, the index ΔPs, the over-limit time ratio p_{out}, and the energy loss index ΔE are shown in Table 2.

It can be seen from Table 2 that in the case where the wind power sharply declines in the short-term, the grid-connection fluctuation of the wind power in Scheme 1 is minimal, and the best flexible grid-connection function is realized.

C. ENERGY CONVERSION PERFORMANCE AND DISCUSSION

Under the typical days and extreme scenarios, the superiority of Scheme 1 for achieving wind power flexible grid-connection control has been proved. Furthermore, based on the comprehensive energy conversion efficiency index defined in Section III, the performance of the wind power grid-connection system is analyzed.

Fig. 9 is obtained according to Section III, and the blue area indicates the operating range of the hybrid energy storage system under different operating conditions.

The curve shown in Fig. 9 is divided into two working areas, A and B, according to the comprehensive efficiency. Point *a* corresponds to Scheme 1 switching from the battery to the hydrogen storage unit in the maximum efficiency mode. Point *b* corresponds to the case where the battery of Scheme 2

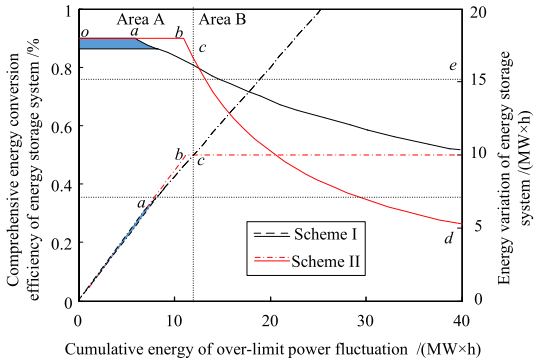

FIGURE 9. The energy conversion efficiency of strategies I and II.

is full. Point *c* corresponds to point when the critical value indexes of Schemes 1 and 2 are the same. In Area A, the hydrogen storage system of Scheme 1 may partially bear the charge/discharge energy of the batteries in Scheme 2, so the comprehensive conversion efficiency and the energy variation of Scheme 1 are not higher than those of Scheme 2. In Area B, the SOC of the batteries in Scheme 2 exceeds the limit, and it no longer participates in dispatching. In the same situation, the hydrogen storage unit in Scheme 1 continues to work, so the convertible energy is large than that in Scheme 2. The difference between the comprehensive conversion efficiency and energy variation of the two schemes sharply increases with the increase in $E_{\Delta P}$. The superiority of the hybrid energy storage system for the wind power flexible grid connection control is obvious.

When the two schemes work at a position near point *c* on typical days, the energy conversion efficiency of the two schemes are close. In the extreme scenario where the wind speed drops continuously, Scheme 1 works in the *c*-*e* section of area B, and the hybrid energy storage unit is turned on at the same time. Although the energy loss is higher when the hydrogen energy storage system participates, the hydrogen energy storage system also improves the power supply continuity of the hybrid energy storage system, which improves the energy conversion efficiency. Therefore, the hybrid energy storage system of Scheme 1 has obvious advantages in improving the reducing wind energy curtailment when the continuous output is needed in extreme scenarios.

To verify the conclusion drawn from Fig. 9, quantitatively analysis of η_{total} is carried out: Four typical days the same as those in table 1, which have different $E_{\Delta P}$, are adopted as input to figure out corresponding $E_{\Delta S}$ and η_{total}, and the results are presented in Table 3.

As shown in Table 3, as for typical day 1, the energy conversion efficiency of scheme 2 seems better than scheme 1 since $E_{\Delta P}$ is less than 12MWh in this case, while the energy conversion efficiency of scheme 1 will be superior to scheme 2 for the else three days, among which $E_{\Delta P}$ is greater than 12MWh. It implies that the continuous support from energy storage system is necessary in these cases. By this means, the advantage of the hybrid energy storage system can be presented clearly. By the way, it can be seen that the

TABLE 3. Energy conversion efficiency comparison between two schemes.

Typical days	Schemes	$E_{\Delta P}$/MW	$E_{\Delta S}$/MW	η_{total}
Typical day 1	Scheme 1	10.7	8.8	82%
	Scheme 2	10.7	10.7	100%
Typical day 2	Scheme 1	23.8	17.5	73.5%
	Scheme 2	23.8	9.9	41.6%
Typical day 3	Scheme 1	16.9	10.9	65.1%
	Scheme 2	16.9	9.9	58.6%
Typical day 4	Scheme 1	25.6	12.5	48.8%
	Scheme 2	25.6	9.9	38.7%

TABLE 4. Effect influenced by the configuration ratio of the hybrid energy storage system.

Battery/MW	Hydrogen storage /MW	ΔP_s/MW	ΔE/(MW·h)
10	0	8.05	7.71
6	2	3.21	7.27
4	3	4.83	7.19
2	4	6.12	7.46

energy conversion efficiency of both schemes are quite low in typical day 4. The reason is that the main functionality of the installed energy storage system is not collecting the abandoned wind power and feeding back to the main grid. The main functionality is to suppress the fluctuation of wind power. Therefore, the index of energy conversion efficiency is not the main concern. In fact, the goal of high energy conversion efficiency like else typical days always can be achieved as soon as enlarging the scale of energy storage system enough. Obviously, it is not economic. Enlarging the scale of energy storage system unreasonably to collect minor electricity does not fit the original purpose to install this system, that is, suppress the fluctuation of integrated wind power.

D. FURTHER DISCUSSION OF THE IMPACT OF THE ENERGY STORAGE SYSTEM RATIO AND THE VALUE OF THE PENALTY FACTOR ON THE PERFORMANCE OF THE OPTIMIZATION MODEL

As previously discussed, when the energy storage system battery/hydrogen storage ratio and the value of the penalty factor are fixed, this paper studies the characteristics and performance of flexible grid-connection auxiliary systems for wind farms. In fact, different energy storage system ratios and penalty factors may affect the performance of the optimization model. This section quantitatively analyzes this.

By selecting the wind power output data on the typical day 1, this paper changes the battery/hydrogen storage ratio of the hybrid energy storage system to run the simulation. The evaluation indexes are shown in Table 4.

It can be seen from Table 4 that the configuration ratio selected in this paper is optimal in terms of the grid-connection over-limit power fluctuation index. In terms of the energy conversion loss, when the proportion of the hydrogen storage system is increased, on the one hand, the wind energy curtailment will be reduced due to the improvement in the power supply continuity. On the other hand, the energy conversion loss of the hydrogen storage system is higher. Under the combined effects of the two factors, the energy conversion loss index is the smallest when the battery/hydrogen energy storage ratio is 4 MW/3 MW. In practice, according to different control needs, the battery/hydrogen storage ratio of the hybrid energy storage system can be flexibly selected.

TABLE 5. Control effect influenced by the penalty factors.

α	β	ΔP_s/MW	ΔE/(MW·h)
0.5	0.8	3.89	6.93
0.5	0.5	3.21	7.27
0.5	0.2	2.99	7.76
0.8	0.5	3.01	7.58
0.2	0.5	3.97	6.86

Similarly, the wind power output data of the typical day 1 are selected. The value of the penalty factor is changed under the condition of the 6 MW battery and 2 MW hydrogen storage system, and the corresponding control strategy evaluation indexes are listed in Table 5.

It can be seen from Table 5 that when β increases or α decreases, the control strategy will use the battery to smooth the fluctuation as much as possible, reducing the energy loss from the hydrogen storage energy. In this way, the hydrogen amount is reduced, causing a continuous reduction in the power supply when the wind power continuously goes down. Meanwhile, the power fluctuation smoothing effect is weakened. When β decreases or α increases, the control strategy will more often use the hydrogen storage system to smooth the fluctuations, and the hydrogen amount increases, improving the power supply continuity. Meanwhile, the power fluctuation smoothing effect is slightly enhanced. In summary, if the requirements for the hybrid energy storage system focus on the fluctuation smoothing function, then β can be appropriately reduced or α can be increased. If the requirements focus on reducing the energy loss and improving new energy utilization, then we can appropriately increase β or decrease α.

V. CONCLUSION

To deal with the existing problem of wind farm oriented energy storage device arrangement, a hybrid energy storage system composed of a battery and a hydrogen energy storage device to smooth the fluctuations of wind power effectively is proposed. The energy conversion characteristics of the hybrid energy storage system to achieve flexible wind power grid-connections and the efficient operation of energy storage systems is also discussed. Some conclusions can be drawn according to the results of theoretical analysis and case study:

i) The proposed hybrid energy storage system can realize the flexible grid-connection function of the wind farm, which is superior to that of the single battery energy storage system.

ii) This system also has the advantage of improving the wind power flexible grid-connection control continuity and improving the wind energy utilization rate.

iii) After increasing the ratio of the hydrogen storage system in the hybrid energy storage system, the over-limit fluctuation index and the energy loss index both decrease first and then increase. Meanwhile, the value of the penalty factor also affects the control result. In the follow-up study, specific optimization strategies for the above-mentioned parameters will be further explored.

REFERENCES

[1] Y. Xiao, H. Chao, and C. Xia, "Research on the problems of wind power grid-connecting," *Adv. Mater. Res.*, vols. 512–515, pp. 640–647, May 2012.

[2] R. Hemmati, S. M. S. Ghiasi, and A. Entezariharsini, "Power fluctuation smoothing and loss reduction in grid integrated with thermal-wind-solar-storage units," *Energy*, vol. 152, pp. 759–769, Jun. 2018.

[3] E. Fagan, S. Grimes, J. McArdle, P. Smith, and M. Stronge, "Grid code provisions for wind generators in ireland," in *Proc. IEEE Power Eng. Soc. Gen. Meeting*, Jun. 2005, pp. 1241–1247.

[4] S. Z. Hassan, H. Li, S. Cagriyener, T. Kamal, G. M. Mufti, M. H. Waseem, and H. Gohar, "Integration and simulation of wind with hydrogen/supercapacitor storage hybrid system," in *Proc. Int. Conf. Electr. Eng. (ICEE)*, Mar. 2017, pp. 1–6.

[5] D. F. Recalde Melo and L.-R. Chang-Chien, "Synergistic control between hydrogen storage system and offshore wind farm for grid operation," *IEEE Trans. Sustain. Energy*, vol. 5, no. 1, pp. 18–27, Jan. 2014.

[6] X. Li, L. Yao, and D. Hui, "Optimal control and management of a large-scale battery energy storage system to mitigate fluctuation and intermittence of renewable generations," *J. Modern Power Syst. Clean Energy*, vol. 4, no. 4, pp. 593–603, Oct. 2016.

[7] P. Yu, X. Liu, Y. Zhang, X. Hu, G. Kong, P. Zhao, Y. Cheng, S. Li, X. Zuo, and S. Sun, "Battery–supercapacitor hybrid energy storage system for wind power suppression based on the turbulence model of wind speed," *J. Eng.*, vol. 2018, no. 17, pp. 1922–1929, Nov. 2018.

[8] X. Li, D. Hui, and X. Lai, "Battery energy storage station (BESS)-based smoothing control of photovoltaic (PV) and wind power generation fluctuations," *IEEE Trans. Sustain. Energy*, vol. 4, no. 2, pp. 464–473, Apr. 2013.

[9] A. Khatamianfar, M. Khalid, A. V. Savkin, and V. G. Agelidis, "Improving wind farm dispatch in the australian electricity market with battery energy storage using model predictive control," *IEEE Trans. Sustain. Energy*, vol. 4, no. 3, pp. 745–755, Jul. 2013.

[10] M. Z. Daud, A. Mohamed, A. A. Ibrahim, and M. A. Hannan, "Heuristic optimization of state-of-charge feedback controller parameters for output power dispatch of hybrid photovoltaic/battery energy storage system," *Measurement*, vol. 49, pp. 15–25, Mar. 2014.

[11] I. Sanchez, A. Ursua, L. Marroyo, and P. Sanchis, "Primary regulation strategies applicable to wind farms coupled with hydrogen production systems," in *Proc. Int. Conf. Clean Electr. Power (ICCEP)*, Jun. 2011, pp. 584–587.

[12] M. Beccali, S. Brunone, P. Finocchiaro, and J. M. Galletto, "Method for size optimisation of large wind–hydrogen systems with high penetration on power grids," *Appl. Energy*, vol. 102, pp. 534–544, Feb. 2013.

[13] M. Ni, M. Leung, and D. Leung, "Energy and exergy analysis of hydrogen production by solid oxide steam electrolyzer plant," *Int. J. Hydrogen Energy*, vol. 32, no. 18, pp. 4648–4660, Dec. 2007.

[14] C. B. Robledo, V. Oldenbroek, F. Abbruzzese, and A. J. M. van Wijk, "Integrating a hydrogen fuel cell electric vehicle with vehicle-to-grid technology, photovoltaic power and a residential building," *Appl. Energy*, vol. 215, pp. 615–629, Apr. 2018.

[15] W. Gan, X. Ai, J. Fang, M. Yan, W. Yao, W. Zuo, and J. Wen, "Security constrained co-planning of transmission expansion and energy storage," *Appl. Energy*, vol. 239, pp. 383–394, Apr. 2019.

[16] A. Cano, F. Jurado, H. Sanchez, M. Castaneda, and L. M. Fernandez, "Sizing and energy management of a stand-alone PV/hydrogen/battery-based hybrid system," in *Proc. Int. Symp. Power Electron. Power Electron., Electr. Drives, Autom. Motion*, Jun. 2012, pp. 969–973.

[17] J. Li, J. Fang, I. Wen, Y. Pan, and Q. Ding, "Optimal trade-off between regulation and wind curtailment in the economic dispatch problem," *CSEE J. Power Energy Syst.*, vol. 1, no. 4, pp. 37–45, Dec. 2015.

[18] B. G. Brown, R. W. Katz, and A. H. Murphy, "Time series models to simulate and forecast wind speed and wind power," *J. Climate Appl. Meteorol.*, vol. 23, no. 8, pp. 1184–1195, Aug. 1984.

[19] K. H. Tan, T. Logenthiran, and W. L. Woo, "Forecasting of wind energy generation using self-organizing maps and extreme learning machines," in *Proc. IEEE Region Conf. (TENCON)*, Nov. 2016, pp. 451–454.

[20] S. M. Zhu, M. Yang, and X. S. Han, "Short-term generation forecast of wind farm using SVM-GARCH approach," in *Proc. IEEE Int. Conf. Power Syst. Technol. (POWERCON)*, Oct. 2012, pp. 1–6.

[21] B. Asghari and R. Sharma, "Cost-aware real-time power management of grid-tied microgrids based on battery life regulation," in *Proc. IEEE Manchester PowerTech*, Jun. 2017, pp. 1–6.

[22] J. Löfberg, "Modeling and solving uncertain optimization problems in YALMIP," *IFAC Proc. Volumes*, vol. 41, no. 2, pp. 1337–1341, 2008.

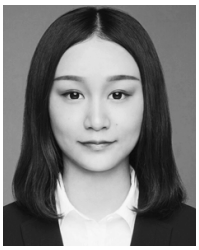

TING WEN was born in Changsha, Hunan, China, in 1992. She received the B.S. and M.S. degrees from the School of Electrical and Electronic Engineering, Huazhong University of Science and Technology, Wuhan, China, where she is currently pursuing the Ph.D. degree.

Her research interests include microgrid planning, energy dispatching strategy of microgrid, and fluctuation smoothing of wind power.

ZHEYUAN ZHANG was born in Hebei, China, in 1994. She received the B.S. and M.S. degrees from the School of Electrical and Electronic Engineering, Huazhong University of Science and Technology, Wuhan, China, in 2016 and 2019, respectively. She is currently a Researcher with Powerchina Hubei Electric Engineering Corporation Limited, Wuhan.

Her researches mainly focus on micro-grid planning.

XIANGNING LIN (Senior Member, IEEE) was born in Guangxi, China, in 1970. He received the M.S. and Ph.D. degrees from the School of Electrical and Electronic Engineering, Huazhong University of Science and Technology (HUST), Wuhan, China.

He is currently a Professor with the School of Electrical and Electronic Engineering, HUST. He has published more than 200 articles in reputed journals/conferences, including 34 articles of the IEEE TRANSACTION and more than 64 articles retrieved by SCI. His research interests are modern signal processing and power system protective relaying.

ZHENGTIAN LI was born in Hubei, China, in 1979. He received the Ph.D. degree from the School of Electrical and Electronic Engineering, Huazhong University of Science and Technology (HUST), Wuhan, China, in 2011.

He is currently an Associate Professor with the School of Electrical and Electronic Engineering, HUST. His researches mainly focus on protective relaying, power system control, and analysis.

CHONG CHEN received the B.S. and the Ph.D. degrees from the School of Electrical and Electronic Engineering, Huazhong University of Science and Technology, Wuhan, China, in 2013 and 2019, respectively.

He is currently an Energy System Engineer with the Changjiang Institute of Survey, Planning, Design, and Research, Wuhan. His research interests include electricity markets, power systems, renewable energy, and stochastic optimization.

ZHIXUN WANG received the B.S. degree from the School of Electrical and Electronic Engineering, Huazhong University of Science and Technology, Wuhan, China, in 2016, where he is currently pursuing the Ph.D. degree in electrical power engineering.

His research interests include microgrid planning and optimization.